1. First Order Approximation to Three-Dimensional Turbulent Boundary Layer and Its Application to Model-Ship Correlation

Ichiro TANAKA*, *Member*, Yoji HIMENO**, *Member*

(*From J.S.N.A. Japan, Vol. 138, Dec. 1975*)

Summary

Three-dimensional turbulent boundary layer equations are expanded according to the ordinary perturbation method with the flat plate flow as the zeroth order solution. The momentum thickness, the local skin friction coefficient and the cross flow angle at the wall including the first order term effects are compared with the measured values on a ship model in acceptable agreement. As applications of this first order solution, an approximate formula to the frictional form factor K_F is obtained and the scale effect of the velocity and vorticity distribution in the boundary layer over ship hulls is discussed.

1. Introduction

To develop the first order perturbation theory of ship boundary layer problems is important and useful for understanding the viscous resistance of ships and the viscous flow around ship forms. The simplest concept along this line is the Froude's idea of the corresponding flat plate. But, following a later development in the boundary layer theory, a variety of treatments of the viscous resistance of ships have been carried out on the basis of this theory. One example would be the hypothesis of the form factor of viscous resistance and the approximate theories based on the two-dimensional or the axi-symmetrical boundary layer equations have been proposed[1)-3)]. Furthermore, recent developments in the field of the three-dimensional boundary layer have made it possible to calculate or to measure the properties of the ship boundary layers. Particularly, it is found that the cross flow angle in the boundary layer plays an important role in the discussion of the stern flow problem, for this quantity would be related closely to the development of the stern bilge vortices. Up to the present time, however, we have had neither a simple approximate formula nor an empirical law for the cross flow angle as well as the frictional resistance on the basis of the three-dimensional turbulent boundary layer theory.

The aim of this study is to obtain the first order perturbation solution of the three-dimensional boundary layer equations taking the flat plate solution as the basic term (zeroth order) of the asymptotic expansion. As the results are expressed in simple forms, some applications to the problem of the frictional form factor and the model-ship correlations of the velocity profiles are possible. These are made in the after part of this paper.

2. First Order Perturbation Solution of Three-Dimensional Turbulent Boundary Layer Equations

In this chapter the formulation of a general integral method for solving the three-dimensional turbulent boundary layer equations is shown, and then the procedure for evaluating

* Osaka University
** University of Osaka Prefecture

the zeroth and the first order solutions according to the regular perturbation of the basic equations is discussed.

To begin with, we take s as the streamline coordinate on the body surface, and n as the equi-potential line coordinate. The momentum integral equations in s and n directions are expressed by eqs. (1) and (2) respectively as follows:

$$\frac{\partial}{\partial s}(U^2\theta_{11})+U\delta_1\frac{\partial U}{\partial s}+\frac{\partial}{\partial n}(U^2\theta_{12})+U\delta_2\frac{\partial U}{\partial n} -K_2U^2(\theta_{12}+\theta_{21})-K_1U^2(\theta_{11}-\theta_{22})=\frac{\tau_s}{\rho} \tag{1}$$

$$\frac{\partial}{\partial n}(U^2\theta_{22})+\frac{\partial}{\partial s}(U^2\theta_{21})-2K_1U^2\theta_{21} -K_2U^2(\theta_{22}-\theta_{11}-\delta_1)=\frac{\tau_n}{\rho} \tag{2}$$

where U represents the outer edge velocity of the layer, τ_s and τ_n the s and n components of the skin friction stress respectively, and ρ the density of the fluid. We take u and v as the velocity components in the s and n directions, and ζ as the normal to the hull surface. The various boundary layer thicknesses δ_1, δ_2, θ_{11} and so on, are defined by:

$$\left.\begin{aligned}
&\delta_1=\int_0^\infty\left(1-\frac{u}{U}\right)d\zeta\,,\qquad \delta_2=\int_0^\infty-\frac{v}{U}d\zeta\,,\\
&\theta_{11}=\int_0^\infty\frac{u}{U}\left(1-\frac{u}{U}\right)d\zeta\,,\\
&\theta_{12}=\int_0^\infty\left(1-\frac{u}{U}\right)\frac{v}{U}d\zeta\,,\\
&\theta_{21}=\int_0^\infty-\frac{uv}{U^2}d\zeta\,,\qquad \theta_{22}=\int_0^\infty-\frac{v^2}{U^2}d\zeta
\end{aligned}\right\} \tag{3}$$

In eqs. (1) and (2), K_1 represents the convergence rate of the streamline and K_2 the geodesic curvature which takes the following form in the streamline coodinates:

$$K_2=\frac{1}{U}\frac{\partial U}{\partial n} \tag{4}$$

In integral methods an auxiliary equation and a skin friction law are usually needed. For simplicity we employ here a general form of the auxiliary equations for two-dimensional flow proposed by Granville[4]:

$$\theta\frac{dH}{ds}=-M\frac{\theta}{U}\frac{dU}{ds}-N\frac{\tau_s}{\rho U^2} \tag{5}$$

where θ can be read as θ_{11} and H as δ_1/θ_{11}. The coefficients M and N are the functions of H, although they are still weakly dependent on R_θ $(=U\theta/\nu)$. As M takes almost the same value for various formulas, we adopt here the following form which can be derived from the two-dimensional energy integral equation.

$$M=H(H-1)(3H-1) \tag{6}$$

On the other hand the coefficient N may take a variety of forms and values as is well known. Considering that it is sufficient for our present purpose to obtain the value N near the flat plate flow condition, and also that the various formulas show similar tendency in Rotta's diagram[5], we can assume the following expression for N, taking account of the equilibrium condition $N=0$ for the flat plate flow $(H=H_0)$ and $N\rightarrow\infty$ for the separating flow $(H=H_{sep})$.

$$N=a\frac{H-H_0}{H_{sep}-H} \tag{7}$$

The coefficient a can be determined by the experimental data for the equilibrium flow. In the present case, substituting a Clauser's data ($H=1.48$ for $\delta_1/\tau_s\cdot dp/ds=2$, where p is the pressure) into eq. (7) with $H_0=1.3$ and $H_{sep}=2.0$, we obtain $a=9.54$. The value N thus obtained becomes close to the value obtained by Buri, Hudimoto or Head's formula in Rotta's diagram.

For the skin friction law in s direction we can employ Ludwieg-Tillmann's formula:

$$\left.\begin{aligned}
&\frac{\tau_s}{\rho U^2}=\alpha(H)(U\theta/\nu)^{-n}\,,\quad \alpha=0.123\times10^{-0.678H}\,,\\
&\qquad\qquad n=0.268
\end{aligned}\right\} \tag{8}$$

The velocity profile is assumed to obey the Mager's model:

$$\left.\begin{aligned}
&\frac{u}{U}=\left(\frac{\zeta}{\delta}\right)^m,\quad v=u\left(1-\frac{\zeta}{\delta}\right)\tan\beta\,,\\
&\tau_n=\tau_s\tan\beta
\end{aligned}\right\} \tag{9}$$

where δ represents the boundary layer thickness and β the cross flow angle at the wall. Then the thicknesses δ_2, θ_{12} and θ_{21} are proportional to $\tan\beta$ and θ_{22} to $\tan^2\beta$.

Now we proceed to the perturbation expansion of these equations. We can assume that the terms containing β, K_1, and K_2, which represent the three-dimensional nature of the boundary layer, are of small order. The deviation of the velocity U from the uniform velocity U_0, and therefore the pressure gradient, is also small, so that U can be expanded in the form:

$$U=U_0+U_1+\cdots \tag{10}$$

The regular asymptotic expansion of the variables θ, H and the friction coefficient c_f may be expressed in the same form as above:

$$\left.\begin{aligned}&\theta=\theta_0+\theta_1+\cdots\,,\quad H=H_0+H_1+\cdots\\ &c_f=c_{f_0}+c_{f_1}+\cdots\,,\quad c_f=2\frac{\tau_s}{\rho U^2}\end{aligned}\right\} \tag{11}$$

The zeroth order equations of these expansions applied to the basic equations are:

$$\frac{d\theta_0}{ds}=\frac{c_{f_0}}{2}\,,\quad \frac{dH_0}{ds}=0\,,\quad c_{f_0}=2\alpha(H_0)(U_0\theta_0/\nu)^{-n} \tag{12}$$

The solution of this equation represents the flat plate flow:

$$\left.\begin{aligned}&U_0\theta_0/\nu=\{\alpha(H_0)\cdot(n+1)\cdot U_0 s/\nu\}^{1/(n+1)}\\ &H_0=\text{const.}\,,\quad c_{f_0}=2\alpha\{\alpha\cdot(n+1)\cdot U_0 s/\nu\}^{-n/(n+1)}\end{aligned}\right\} \tag{13}$$

We can further derive the frictional resistance coefficient C_{F_0} analogous to the Prandtl's formula:

$$C_{F_0}=2\frac{\theta_0}{s}=c_{f_0}(n+1)=\text{const.}\times\left(\frac{U_0 s}{\nu}\right)^{\text{const.}} \tag{14}$$

Now let us obtain the first order perturbation equations considering that all of the terms containing β, K_1, K_2 and the pressure gradient are the first order small quantities. The first order perturbation terms of the expansion of the momentum equation (1) in s direction can be written in the form:

$$U_0^2\frac{\partial\theta_1}{\partial s}+U_0\theta_0(H_0+2)\frac{\partial U_1}{\partial s}+U_0^2\frac{\partial\theta_{12}}{\partial n}-K_1\theta_0U_0^2=\frac{c_{f_1}}{2}U_0^2 \tag{15}$$

Similarly eq. (2) in n direction is expanded as

$$\frac{\partial\theta_{21}}{\partial s}+K_2\theta_0(H_0+1)=\beta\frac{c_{f_0}}{2} \tag{16}$$

where the cross momentum thickness θ_{21} is derived from substituting the velocity profile law into eq. (3) as follows:

$$\theta_{21}=\beta\theta\cdot\lambda(H)\,,\quad \lambda(H)=\frac{-2}{(H-1)(H+2)} \tag{17}$$

The first order term of the thickness θ_{21} is determined by replacing H and θ by H_0 and θ_0 in the eq. (17). The auxiliary equation becomes,

$$\left.\begin{aligned}&\theta_0\frac{dH_1}{ds}=-M(H_0)\cdot\frac{\theta_0}{U_0}\frac{dU_1}{ds}-N'(H_0)H_1\frac{c_{f_0}}{2}\\ &\text{where,}\\ &N(H_0)=0\,,\quad N'(H_0)=\left.\frac{dN}{dH}\right|_{H=H_0}\end{aligned}\right\} \tag{18}$$

The skin friction law takes the form:

$$c_{f_1}=c_{f_0}\left\{-0.678(\ln 10)H_1-n\frac{U_1}{U_0}-n\frac{\theta_1}{\theta_0}\right\} \tag{19}$$

Although these first order perturbation equations (15) to (19) are linear, it is still difficult to obtain an exact solution. Therefore we try here to find an approximate solution. Considering the properties of the first order solution, we can obtain a solution for the cross flow angle β from eqs. (16) and (17) using the initial condition $\beta=0$ at the starting point $s=0$:

$$\beta=\frac{(H_0+1)}{-\lambda(H_0)}\cdot\frac{1}{\theta_0^{\alpha_1}}\int_0^s K_2\theta_0^{\alpha_1}ds\,,\quad \alpha_1=\frac{1-\lambda(H_0)}{\lambda(H_0)} \tag{20}$$

In eq. (20) we can express θ_0 by a function of c_{f_0}, and further replace c_{f_0} by C_{F_0}, i.e. the mean value of c_{f_0}. Then we have

$$\left.\begin{aligned} &\beta=\alpha_2\cdot\frac{1}{s^{\alpha_1}}\int_0^s K_2 s^{\alpha_1}ds \\ &\alpha_1=\frac{H_0}{2}(H_0+1) \\ &\alpha_2=\frac{1}{2}(H_0-1)(H_0+1)(H_0+2)(n+1)^{\alpha_1} \end{aligned}\right\} \tag{21}$$

If we assume that $H_0=1.3$, then $\alpha_1=1.50$ and $\alpha_2=1.63$. When the initial value is given as $\beta=\beta_0$ at $s=s_0$, we must add the damping term $\beta_0(s_0/s)^{\alpha_1}$ to eq. (20) and change the lower limit of the integral to $s=s_0$.

Next we consider H_1, the deviation of the value of the shape factor H from H_0, which is affected mainly by the pressure gradient, as is seen in eq. (18). Neglecting the upstream history as in the two-dimensional case, we have a solution for H_1:

$$H_1=\alpha_3(H_0)\frac{\theta_0}{c_{f_0}}\frac{1}{U_0}\frac{dU_1}{ds}, \quad \alpha_3=-2\frac{M(H_0)}{dN(H_0)/dH_0} \tag{22}$$

It is obvious that we can solve eq. (18) exactly, but we could obtain a similar expression to eq. (22) through expanding the exact solution and neglecting the higher order terms of the derivatives of U_1. For simplicity, we adopt here the expression (22). The value of the coefficient α_3 is about -0.166 for $H_0=1.3$.

On the other hand, the momentum thickness is influenced by the upstream condition. From eqs. (15), (19) and (22) we can derive the expression for θ_1 assuming that the effect of $\partial/\partial n$ is negligible in the average:

$$\left.\begin{aligned} &\frac{\theta_1}{\theta_0}=\alpha_4\frac{1}{s}\int_0^s\frac{U_1}{U_0}ds+\alpha_5(H_0)\frac{1}{s}\int_0^s\frac{s}{U_0}\frac{dU_1}{ds}ds \\ &\qquad+\frac{1}{s}\int_0^s K_1 s ds \\ &\alpha_4=-\frac{n}{n+1}, \quad \alpha_5=-H_0-2-0.339(\ln 10)\alpha_3(H_0) \end{aligned}\right\} \tag{23}$$

and also for c_{f_1} from eqs. (19), (22) and (23).

Thus we have obtained all the first order perturbation solutions of the boundary layer quantities. In this solution the terms of the increase of the outer edge velocity, the pressure gradient, the streamline convergence and the curvature appear explicitly, so that we can easily acquire a clear understanding on their effects. Particularly, it may be of interest that the quantities θ_1, H_1 and c_{f_1} are not affected by the streamline curvature K_2, but, on the contrary, the cross flow angle β is determined mainly by K_2.

Now some comparisons of these solutions with the experimental results are made. For the experimental data, we quote here the results of the model test of SSPA cargo ship form carried out by Larsson[7]. Fig. 1 shows

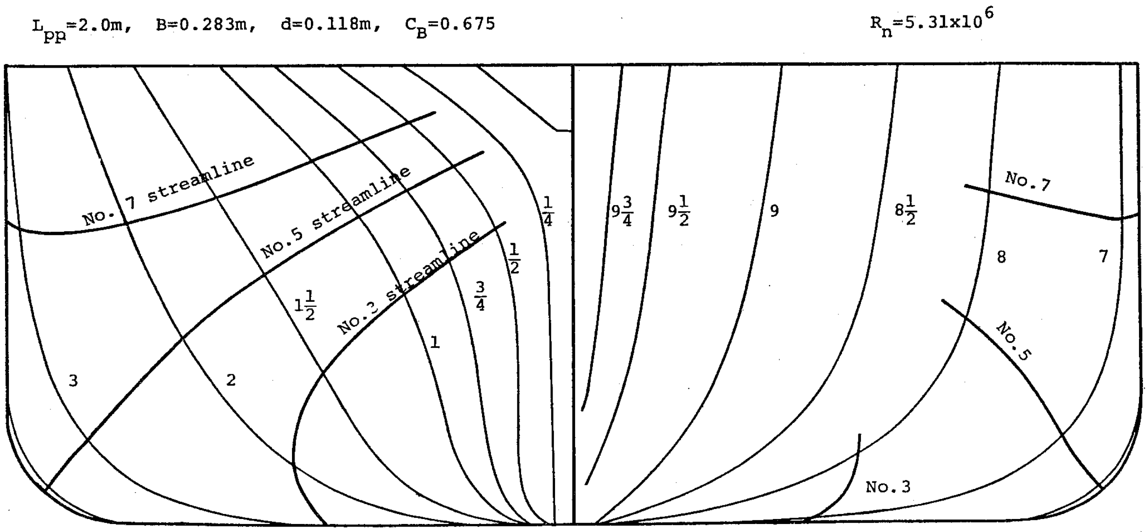

Fgi. 1 Body plan and streamlines of SSPA cargo ship model given by Larsson

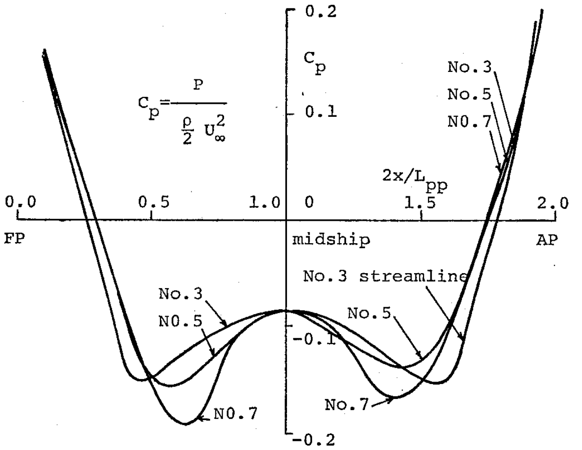

Fig. 2 Pressure distribution along streamlines calculated by Larsson

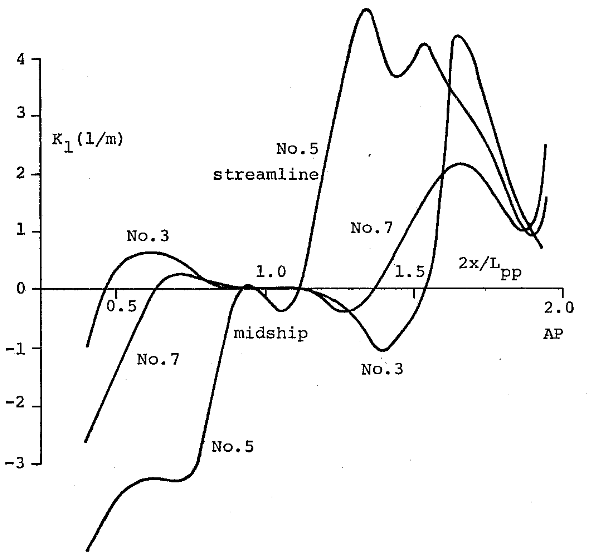

Fig. 3 Streamline convergence K_1 given by Larsson

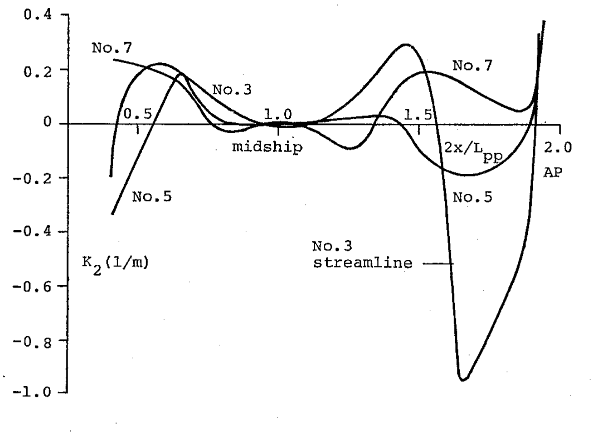

Fig. 4 Geodesic curvature K_2 of streamlines given by Larsson

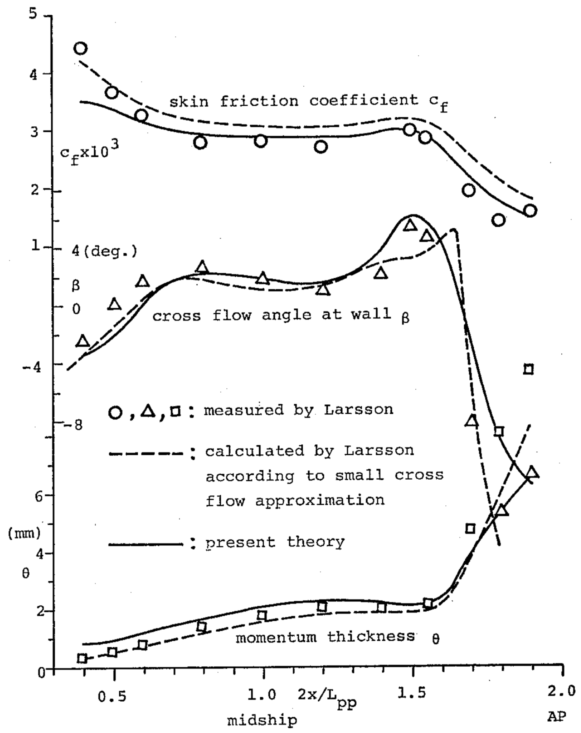

Fig. 5 Boundary layer solutions along No. 3 streamline

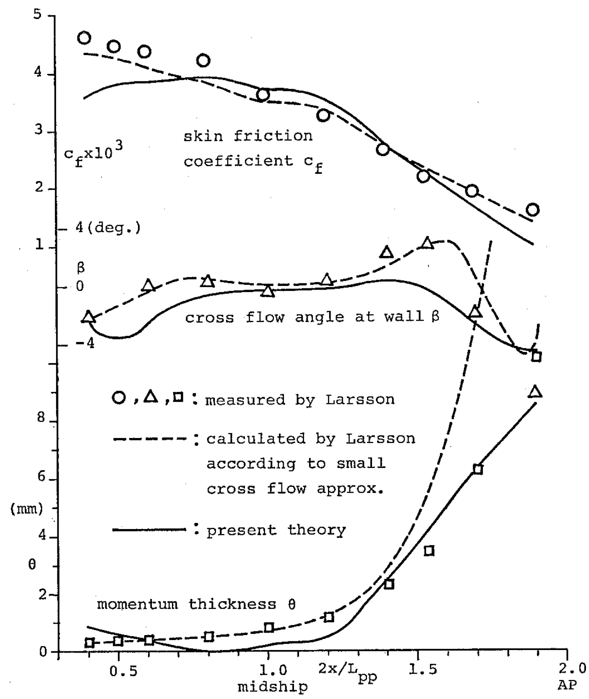

Fig. 6 Boundary layer solutions along No. 5 streamline

the body plan, the particulars of the model, the streamline and Reynolds number. Larsson gave the distributions of pressure (Fig. 2), the convergence K_1 (Fig. 3) and the curvature K_2 (Fig. 4) along streamlines. Using these values, we can calculate the solution by the present method with the condition that the starting point is at SS 8, and zeroth order solutions θ_0 and c_{f_0} are derived from Schoenherr's formula for the flat plate, using $H_0=1.3$. Figs. 5 to 7 show the distributions of θ, c_f and β along the streamlines Nos. 3, 5 and 7 respectively, including the results of Larsson's calculations in which the assumption of small cross flow and the entrainment rate equation are used. In these figures some influences of using the flat plate value at the initial station appear on θ and c_f, while the negative convergence rate of No. 5 streamline causes a decrease in θ. On the whole, however; we can conclude that the agreement between the present solutions and the measured values is fairly good and it is expected that the discrepancy between them will decrease with the use of an appropriate initial condition.

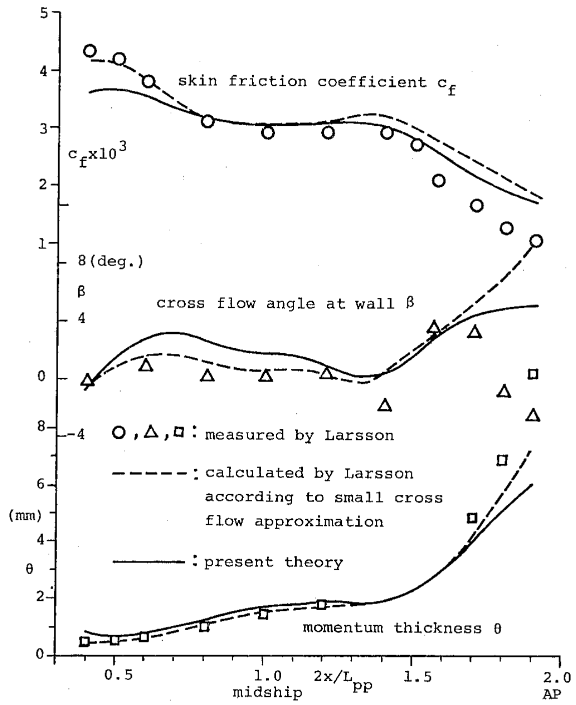

Fig. 7 Boundary layer solutions along No. 7 streamline

3. Frictional Form Factor

As an application of the first order approximate solution, we can consider a simple formula for the frictional form factor K_F, which is a part of the form factor K. Sasajima *et al.*[8] proposed a theoretical formula for K_F about seventeen years ago:

$$K_F=\frac{1}{S}\int\frac{U^2-U_0^{\ 2}}{U_0^{\ 2}}d\sigma \tag{24}$$

where S denotes the wetted surface area and $d\sigma$ is surface area element, and the integral is taken over the whole wetted area of the hull. The value of K_F of eq. (24) has been considered to be reasonable or sometimes slightly high. Here, we compare the value with the one deduced from the first order approximate solution.

The frictional resistance coefficient C_F can be expanded up to the first order small terms in the form,

$$\begin{aligned} C_F&=\frac{2}{\rho S U_0^{\ 2}}\iint \tau_s ds dn \\ &\fallingdotseq\frac{1}{S}\iint (c_{f_0}+c_{f_1})\left(1+2\frac{U_1}{U_0}\right)ds dn \end{aligned}\tag{25}$$

where we can consider that s and n axes lie approximately in the longitudinal and the girthwise directions respectively. Eq. (25) can be written in the form,

$$\begin{aligned} K_F&=\frac{C_F-C_{F_0}}{C_{F_0}}=\frac{1}{C_{F_0}S}\iint c_{f_0}\frac{2U_1}{U_0}ds dn \\ &+\frac{1}{C_{F_0}S}\iint c_{f_1} ds dn\equiv K_{F_1}+K_{F_2} \end{aligned}\tag{26}$$

When integrating the first term, we can replace c_{f_0} in the integrand by C_{F_0}, the mean value of c_{f_0}, so that we obtain the same expression as eq. (24):

$$K_{F_1}\fallingdotseq\frac{1}{S}\iint\frac{2U_1}{U_0}ds dn\fallingdotseq\frac{1}{S}\iint\frac{U^2-U_0^{\ 2}}{U_0^{\ 2}}ds dn \tag{27}$$

K_{F_1} represents only the influence of the velocity increment over the hull.

The second term K_{F_2}, including the effect of variation of c_f, becomes negative after integrating eq. (19) over the hull. Here we assume that the integration of U_1 along n axis is replaced by the girthwise mean value and that the girth length $b(s)$ at any station can be expanded as follows:

$$\left.\begin{aligned} & b(s)=b_0+b_1(s)+\cdots \\ \text{where} & \\ & b_0=\frac{1}{L}\int_0^s b(s)ds=\frac{S}{L}, \end{aligned}\right\} \tag{28}$$

and L is the ship length. Then the convergence K_1 becomes approximately

$$K_1=-\frac{1}{b}\frac{db}{ds}\doteqdot-\frac{1}{b_0}\frac{db_1}{ds} \tag{29}$$

We can finally obtain the expression for K_{F_2} in the form

$$K_{F_2}=0.209K_{F_1}+\frac{0.453}{S}\iint\frac{U^2-U_0^2}{U_0^2}\ln\left(\frac{s}{L}\right)dsdn$$
$$+0.164\left(\frac{\bar{U}_1}{U_0}\right)_{s=L}-\frac{0.268}{S}\int\left(b-\frac{S}{L}\right)\ln\left(\frac{s}{L}\right)ds \tag{30}$$

The third term represents the girthwise average of the velocity variation at the stern. The numerical coefficients are calculated for $H_0=1.3$. (The effect of the value of H_0 will be discussed in the next chapter.) Thus we can calculate the value of K_F through eqs. (26), (27) and (30), once the pressure distribution on the hull and the girth length variation are given. It may occur that the value of $\bar{U}_1$ at the stern becomes singular in potential flow. In this case it is necessary to estimate the value by extrapolating the upstream values to that station, or to exclude the stern region in the numerical integration of eq. (30).

Now we proceed to the comparison of the calculated results with the experimental values. The used ship forms are the Lucy Ashton of BSRA[9], a parent form of Todd Series 60 with $C_B=0.70$[10], a tanker form M684[11] in Moor's study and a tanker form M167 of SR98 in Japan[12]. The inviscid velocity on the hull was calculated by means of Hess and Smith's method. Table 1 shows the values of K_F calculated by the present theory and the experimental values of K_F for the Lucy Ashton and the Moor's tanker form measured by Joubert and Matheson[13),14)] in a wind tunnel. The values of K from resistance tests are also given in the table. Here all values are based on the Schoenherr's line, and the term "exact cal." means the values calculated by means of an exact integral method developed recently by the authors[15].

Table 1 Analysis of frictional form factor of models

ship name	L. Ashton	Ser. 60	Moor M684	M167
C_B	0.685	0.700	0.800	0.802
$R_n\times10^{-6}$	4.53	1.30	6.63	3.08
K_{F_1}, present cal.	−0.001	0.040	0.064	0.080
K_{F_2}, present cal.	−0.122	−0.070	−0.050	−0.070
$1+K_F$, present cal.	0.878	0.970	1.014	1.010
$1+K_F$, exact cal,	1.058	1.056	1.065	1.073
$1+K_F$, experiment	1.006	—	1.018	—
$1+K$, experiment	1.071	1.097	1.362	1.320

The values of K_F of the present first order theory are smaller than the values of K_{F_1} in all cases, being almost zero or negative. This situation will not change if the viscous modification is applied to the potential flow velocity distribution at the stern. The experimental value of the tanker form M684 agrees well with the values by the present theory while the experimental value of the Lucy Ashton is very small compared with the present calculation. Furthermore, considering the fact that, in an experiment conducted at Osaka University[16], the frictional resistance coefficient obtained through subtracting the pressure resistance coefficient from the total resistance coefficient was smaller than the Schoenherr's line, and also that Namimatsu *et al.*[17] obtained similar results, we may safely conclude that K_F is very small even in tanker forms and the values of the first order theory is probably reasonable.

On the other hand, the values of the "exact calculation" are nearly the same in all cases although slight increase with C_B is noticed.

To inquire into the validity of these values we have to discuss the distribution of the skin friction but the detailed discussion will be left to another paper by authors[15]. Here we only point out that the author's exact solution shows slightly higher values of the skin friction than the measured ones at the stern by a few percent in the value of $1+K$, which is probably caused by the auxiliary equation used in the "exact method". In the present theory we use a different form of the auxiliary equation, therefore correspondency between two methods is not necessarily complete.

4. Scale Effect

We can discuss the scale effects of the boundary layer parameters and the viscous flow at the stern considering the characteristics of the first order perturbation solution obtained above. In the first place it is concluded that the quantities β, H, θ_1/θ_0 and c_{f_1}/c_{f_0} are not affected by the change of the ship scale and K_F is independent of Reynolds number R_n. This is clear from simple inspection into the nature of the zeroth order solution, *i.e.* H_0=const. and $\theta_0/L\propto c_{f_0}\propto C_{F_0}$, shown in eqs. (12), (13) and (14). These conclusions are probably true provided that the variation of R_n is not large. In the ship problem, however, we need to consider correlation problems with more wider range of R_n, hence we can not assume H_0=const. any more. With the variation of R_n from model to ship, the value of H_0 changes from about 1.4 to 1.1. Therefore the quantity such as $H-1$ in eq. (17) suffers from the direct influence of the variation of H_0, while $H+2$ in the momentum integral equation does not vary much. To exactly discuss the scale effect including the variation of H_0, we need to proceed to the second order solution, but this remains to be solved. Here we consider the scale effect by investigating the change caused by the variation of H_0 within the first order solution.

At the beginning let us consider the cross flow angle β. From eq. (21), the coefficient α_2 is affected by H_0 variation, but the value α_1 does not change much with R_n. We can express α_1 and α_2 as functions of C_{F_0} with the aid of Schoenherr's formula and Ludwieg-Tillmann's law as shown in Fig. 8, *i.e.*

$$\alpha_1 \fallingdotseq 1+150C_{F_0}\,, \qquad \alpha_2 \fallingdotseq 535C_{F_0} \tag{31}$$

Hence β is almost proportional to C_{F_0}. In Fig. 9 we show the calculated results of the girthwise distribution of β at SS 1/2 of the model M 167 by the exact integral method[15]. In the figure we plot also the estimated curves of β at high R_n from the value at a low R_n assuming that $\beta\propto C_{F_0}$. These curves do not differ

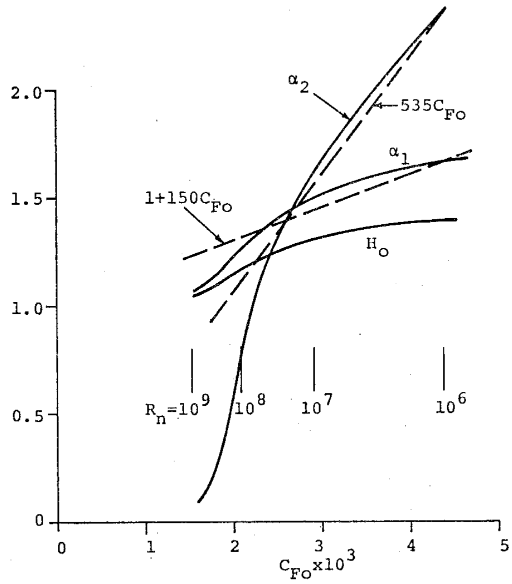

Fig. 8 Coefficients α_1 and α_2 in the formula of cross flow angle at the wall β

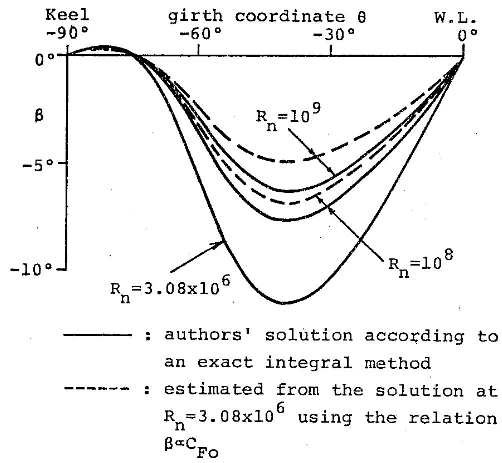

Fig. 9 Distribution of cross flow angle β at SS 1/2 of a tanker model M 167

much from the exact values, although, to be more exact, we notice that $\beta\propto C_{F_0}^{0.5}\sim C_{F_0}^{1.0}$. Hence, for practical purposes, we can consider $\beta\propto C_{F_0}$.

To study the effect of scale on other quantities, the auxiliary equations (5), (6) and (7) should be valid for all R_n. Though the coefficient M in eq. (6) may be independent of R_n, the scale effect of the coefficent N in eq. (7) is difficult to assess because of the non-uniqueness of its value when determined from the experimental data. Thus the scale effect of H_1 is unknown for it contains $M/(dN/dH_0)$. The scale effect of c_{f_1}/c_{f_0} and the part of K_F which is influenced by pressure gradient are both unclear because they contain H_1. On the other hand, θ_1/θ_0 does not depend on R_n variation.

Next let us discuss the velocity profiles. In s direction, we have already assumed the power law in eq. (9):

$$\frac{u}{U}=\left(\frac{\zeta}{\delta}\right)^m,\quad \delta=\frac{H(H+1)}{H-1}\theta,\quad m=\frac{H-1}{2} \tag{32}$$

Within the first order approximation and for geometrically similar ship forms, $\theta\propto\theta_0\propto C_{F_0}L$, and also $\delta/L\propto\sqrt{C_{F_0}}$ since $(H-1)/H\propto\sqrt{c_{f_0}}$ (if the logarithmic velocity profile is assumed, we have $\delta/L\propto C_{F_0}^{0.65}$). The parameter m, however, decreases with R_n so that the value of u/U increases at the corresponding point of ζ/δ. Therefore, taking account of both effects, we may safely consider that $\delta/L\propto C_{F_0}$ with constant m for both the model and the actual ship condition. This result is the same as the one by Sasajima *et al.*[18] on the contraction law for velocity profile.

For the crosswise velocity v/U, the similar contraction law in the ratio of C_{F_0} holds for the corresponding points between the model and the ship. However in this case it should be noted that the value of the velocity v/U will also decrease by the ratio of C_{F_0} because $\beta\propto C_{F_0}$ as shown in the preceeding paragraph.

The velocities (u, v) can be transformed into (V_x, V_y, V_z), the components in the directions of the body coordinates (x, y, z), where x is in longitudinal direction, and y and z lie in the cross sectional plane of the ship. Then we have

$$V_x=v\left(\frac{\zeta}{\delta}\right)\cos(n, x)+u\left(\frac{\zeta}{\delta}\right)\cos(s, x) \tag{33}$$

Because the first term can be neglected, we have

$$V_x\fallingdotseq u\left(\frac{\zeta}{\delta}\right)\cos(s, x) \tag{34}$$

Thus the contraction law for V_x is the same for u. This is approximately supported by the experimental data of SR107[19] and by Namimatsu and others[20].

Next, in y and z directions we have

$$\left.\begin{aligned} V_y&=v\left(\frac{\zeta}{\delta}\right)\cos(n, y)+u\left(\frac{\zeta}{\delta}\right)\cos(s, y)\\ V_z&=v\left(\frac{\zeta}{\delta}\right)\cos(n, z)+u\left(\frac{\zeta}{\delta}\right)\cos(s, z)\end{aligned}\right\} \tag{35}$$

where the first and the second terms are of the same order and can not be neglected. Further the scale effects of the velocities u and v are different from each other, so that we can not contract simultaneously both values of V_y and V_z in the same ratio in ζ direction. Noting that u remains at the outer edge of the boundary layer while v vanishes there, we can separate the velocity components into two parts: one is the part of V_y (or V_z) which remains at the outer edge of the layer and is proportional to u distribution. This part obeys the same contraction law as u. The other part is the rest which corresponds to v component. Namimatsu *et al.*[20] measured the flow angles $V_y/V_x\,(=\beta_H)$ and $V_z/V_x\,(=\beta_V)$ as shown in Fig. 10. In this case, the deviations from the edge values may be regarded as the distribution of v/u, hence the contraction in the ratio of C_{F_0} both in the normal direction to the hull and in the value of v/u is necessary. Fig. 10 contains also the estimated values by the Namimatsu's method of contraction taking account of only the y direction (*i.e.* approximately ζ direction), which seems to show the existence of some error near the wall. Hence it will be realized that the second contraction in v is needed for β_V,

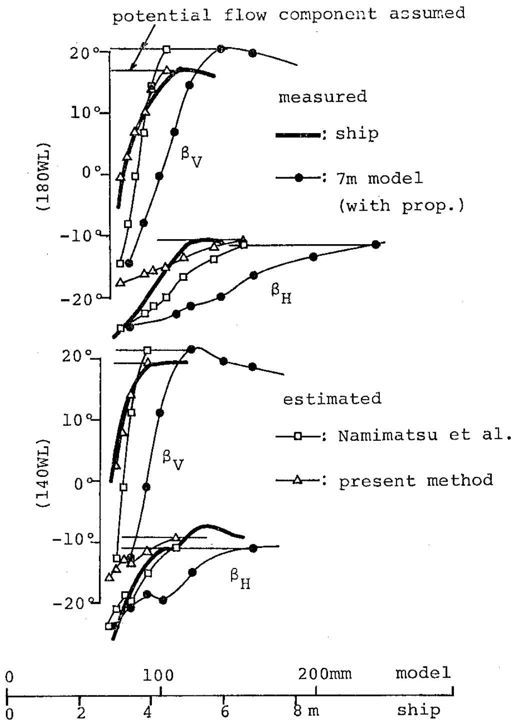

Fig. 10 Distribution of vertical and horizontal cross flow angles (β_V and β_H) at SS 0.45 of a tanker model measured by Namimatsu *et al.* in full load condition

the cross flow angle in this case. On the contrary, for the value of β_H, which corresponds to the normal flow angle to the wall in this case, the present contraction method seems not to be valid. This point should be studied in detail in the future. Here we only point out, on the basis of the boundary layer approximation, that the streamwise and the crosswise velocities obey different laws for the scale effect.

As an extension of the contraction law of the velocity profiles, we can discuss the scale effect of the longitudinal (bilge) vortices at the stern from the standpoint of the boundary layer theory. For this purpose it will be necessary to provide an evidence that it is possible to deal with the bilge vortex as a type of the cross flow in the boundary layer, but this is not possible now. Instead, we only point out the following two facts. i) The bilge vortex lies actually inside the boundary layer. ii) The boundary layer approximation has been applied successfully to the analysis of the wing tip vortex. Anyway we can express the longitudinal vortex flow by the vorticity ω_x, the axis of which is in x direction. From eq. (35) we have

$$\omega_x = A\frac{\partial v}{\partial \zeta} + B\frac{\partial u}{\partial \zeta} = A\cdot\frac{U\beta}{\delta}f_1\left(\frac{\zeta}{\delta}\right) + B\frac{U}{\delta}f_2\left(\frac{\zeta}{\delta}\right) \tag{36}$$

where the first term of the right hand side represents the component of the cross flow, and the second term the component of the main flow. The coefficients A and B depend solely on the ship form and the location, hence they are not affected by the scale. Near the stern the two terms in eq. (36) become of the same order of magnitude. Considering that $\delta/L \propto C_{F_0}$ and $\beta \propto C_{F_0}$, the value of ω_x grows with decreasing C_{F_0} on account of the second term, because Af_1 and Bf_2 have the same sign in the case when the bilge vortices exist. Further, the ratio of the first term to the second is not uniform in the girth direction. Besides, the second term is influenced by the flow angle at the outer edge of the layer which might alter between the model and the ship due to the effect of the displacement thickness. Therefore the contraction rate of the magnitude of the vorticity ω_x can not be simply decided even within the boundary layer approximation, although the shape of the vorticity contour of the actual ship can be roughly estimated by the simple contraction of the contour in the model with the ratio of C_{F_0}, because the shape of the vorticity contour is mainly characterized by the first term. Finally let us add a little discussion on the circulation Γ, which is given by

$$\Gamma = \int \omega_x ds \propto U_\infty L(A'\beta + B') \tag{37}$$

where ds is the elementary area and the area of integration is assumed to be proportional to $L\delta$. The first term is due to the cross flow and β is taken as the mean value in the sectional plane. The second term is the projected part along x axis. (This expression is obtained by assuming that Γ of the longitudinal vortex is approximately treated by excluding the regions near the wall and near the edge of the boundary layer.) Hence the value of Γ for the ship seems to be smaller than the value for the model, but we can not conclude this quantitatively due to the variation of the coefficients A' and B'.

5. Conclusions

The first order perturbation solution is obtained through the expansion of the three-dimensional boundary layer equations with the flat plate as the zeroth order solution. The conclusions are;

i) The first order perturbation solutions for the boundary layer parameters agree fairly well with the experimental data.

ii) The frictional form factor K_F derived from the first order solutions is considerably small as compared with the existing formula, but the present value is rather close to the experimental one.

iii) The cross flow angle β is nearly proportional to the frictional resistance coefficient C_{F_0} of the corresponding flat plate. To obtain the cross flow velocity distribution in the actual ship from the model, not only the contraction of the distribution in the direction of the normal to the hull but also that of the magnitude of the cross flow velocity in the ratio of C_{F_0} are required.

iv) The shape of the longitudinal vorticity component contour of the ship can be obtained by simply contracting the contour in the model in the ratio of the values of C_{F_0} for the ship and the model, although the scale effect of the magnitude of the vorticity is complicated because of the difference of the contraction laws between the main flow and the cross flow.

Aknowledgment

The authors express their heartfelt gratitude to Prof. Em. Hideo Sasajima, Osaka University, for his valuable discussions, and to Prof. Norio Tanaka, University of Osaka Prefecture, Mr. Toshio Suzuki, Lecturer, Osaka University and Mr. Taketoshi Okuno, Assistant, and Mr. Shigeru Hayashita, graduate student, University of Osaka Prefecture for their various assistance in the present research.

A part of this study was supported by the Scientific Research Fund of the Ministry of Education. The computers at Kyoto University and at University of Osaka Prefecture were used for the calculations.

References

1) I. Tanaka: Form Effects on Viscous Resistance of Ships, Part I and II, J.S.N.A. Japan, Vol. 113, pp. 7–16 (1963) and Vol. 114, pp. 34–43 (1963) (both in Japanese), available in English in Selected Papers, J.S.N.A. Japan, Vol. 3 pp. 19–39 (1969)
2) H. Sasajima and I. Tanaka: Form Effects on Viscous Resistance and Their Estimation for Full Ships, Proc. 10th ITTC, pp. 122–128 (1963)
3) P.S. Granville: A Modified Froude Method for Determining Full-Scale Resistance of Surface Ships from Towed Model, J.S.R., Vol. 18 No. 4 pp. 215–223 (1974)
4) P.S. Granville: Integral Methods for Turbulent Boundary Layers in Pressure Gradients, N.S.R.D.C. Rep. 3308 (1970)
5) J.C. Rotta: Progress in Aeronautical Sciences, ed. by A. Ferri *et al.*, Vol. 2 p. 202 (1962)
6) F.H. Clauser: See J.C. Rotta[5], p. 124
7) L. Larsson: Boundary Layers of Ships, Part I to IV, SSPA Allman Rep., Nr. 44 to 47 (1974)
8) H. Sasajima *et al.*: Form Effect on Frictional Resistance of Ships and Power Prediction of Large Tankers, J.S.N.A. Japan, Vol. 103 pp. 211–222 (1958) (in Japanese)
9) J.F.C. Conn *et al.*: BSRA Resistance Experiments on the Lucy Ashton, T.I.N.A., Vol. 95 pp. 350–436 (1953)
10) F.H. Todd *et al.*: Series 60-The Effect upon Resistance and Power of Variation in Ship Proportions, T.S.N.A.M.E., Vol. 65 pp. 445–589 (1957)
11) D.I. Moor: The © of Some 0.80 C_B Forms, T.R.I.N.A., Vol. 102 pp. 93–152 (1960)
12) The Shipbuilding Research Association of Japan: SR98, Rep. No. 61 (1967) (in Japanese)
13) P.N. Joubert and N. Matheson: Wind Tunnel Tests of Two Lucy Ashton Reflex Geosims, J.S.R., Vol. 14 No. 4 pp. 241–276 (1970)
14) N. Matheson and P.N. Joubert: Experimental Determination of the Components of Resistance

of a Small 0.80 C_B Tanker Model, J.S.R., Vol. 17 No. 3 pp. 162–180 (1973)

15) Y. HIMENO and I. TANAKA: An Exact Integral Method for Solving Three-Dimensional Turbulent Boundary Layer Equations around Ship Hulls, J.K.S.N.A. Japan, Vol. 159 pp. 65–73 (1975) (in Japanese), available in English in Technol. Rep. Osaka Univ., Vol. 26 No. 1332 (1976)

16) H. SASAJIMA *et al.*: Pressure Distribution on Full Form Hull, unpublished (1969)

17) M. NAMIMATSU *et al.*: Measurement of Hull Surface Pressure (Part 2), J.T.T.C., No. 36–13 (1975) (in Japanese)

18) H. SASAJIMA *et al.*: Wake Distribution of Full Ships, J.S.N.A. Japan, Vol. 120 pp. 1–9 (1966) (in Japanese)

19) The Shipbuilding Research Association of Japan: SR107, Rep. No. 142 (1972) (in Japanese)

20) M. NAMIMATSU *et al.*: Wake Distribution of Ship and Model on Full Ship Form, J.S.N.A. Japan, Vol. 134 pp. 65–74 (1973) (in Japanese)